Iranian Polymer Journal
15 (8), 2006, 667-674

Availlable online at: http://journal.ippi.ac.ir

Finite Element Analysis of the Steel-Belted Radial Tyre with Tread Pattern under Contact Load

Mir Hamid Reza Ghoreishy

Department of Rubber, Faculty of Polymer Processing, Iran Polymer and Petrochemical Institute, P.O. Box: 14965/115, Tehran, Iran

Received 23 May 2006; accepted 5 August 2006

ABSTRACT

This paper addresses the finite element modelling of a steel belted radial tyre under static contact load using ABAQUS code. The model combines the 3D parts of the complex tread patterns and the quasi axisymmetric part of the tyre in which the tread blocks are not included. These two sections were meshed separately and linked together using a tying algorithm implemented in the code. The fibber reinforced parts of the tyre including ply, belts, and cap ply were modelled using rebar layer embedded in the surface elements. A hyperelastic material model was used in conjunction with a linear elastic one to describe the stress-strain behaviour of rubber and reinforcing fibres, respectively. The developed model was used to simulate the 175/70R14 steel-belted radial tyre subjected to inflation and contact loads. Three belts angles were selected to examine the effect of belt angle variations on the mechanical behaviour of the tyre. In addition, the results were also compared with a similar tyre model in which a simply ribbed tread was used instead of complex tread pattern. The friction between tread surface and contact road surface was simulated using the Coulomb's friction law. The numerical results and also the comparison of experimentally measured tyre deflection under concentrated vertical load revealed that neglecting the details of the tread blocks has very minor effect on the predicted tyre deformation. However, differences can be large enough when considering secondary or higher variables such as contact pressure, stress, and strain energies. It is also shown that a belt angle of 20° is the best comprised value among the selected design parameters.

Key Words:

finite element method;
radial tyre;
tread pattern;
strain energy;
contact pressure.

INTRODUCTION

Finite element analysis of car tyres in different loading conditions is generally based on the results of their static analysis under contact load. For example, a modal analysis for the prediction of natural frequencies and mode shapes or steady state rolling analysis should be performed after evaluating the tyre shape in contact load. Consequently, development of a valid and accurate finite element model for the prediction of the stresses and strains under contact (footprint) load is of prime importance. In past, many researchers have tried to model the deflection of a pneumatic tyre under static contact load and in this regard, a number of numerical algorithms have been developed so far [1-6]. Traditionally, finite element analysis of tyres for static loading is carried out based on the use of axisymmetric tread in which the complex shapes of the blocks in tyre tread (specially for

To whom correspondence to be addressed.
E-mail: m.h.r.ghoreishy@ippi.ac.ir

radial passenger car tyres) are replaced by a smooth or simply ribbed solid part. There are two main reasons for this approximation as follows:

i) Difficulty in developing the refined and computationally efficient finite element mesh for tread blocks.

ii) Highly computational cost and effort which require huge hardware and memory resources to run a complex tyre model with detailed tread area.

However, needless to say, neglecting the tread blocks pattern gives rise to errors in numerical predictions of tyre behaviour in contact load. There are two methods to tackle this problem. The first method is the global/local analysis. In this technique a global method is first adopted in which a full 3D model is developed and the finite element analysis of the structure with a relatively coarse mesh is performed. Then a part of the structure around the contact area is separated and meshed with pattern of tread blocks (local model). The interpolated displacements computed from global method are applied to the local model as the prescribed boundary conditions. This technique ignores the interactions between tread blocks and carcass (especially at belt packages) and thus cannot predict tyre behaviour correctly [7]. The second approach is based on the development of a full 3D model with detailed tread blocks inserted directly in the model. Although the latter method needs larger computational time and resources, due to the advances in geometrical and finite element modeling as well as computer technology this is not a difficult task and can be carried out using the existing hardware and software.

In this paper we have described a finite element model developed for the simulation of the contact of the 175/70R14 steel-belted radial tyre with tread blocks pattern directly incorporated into the model. Finite element mesh of the tyre body (excluding tread pattern) was first created and then assembled with generated elements of tread blocks. These two meshes were linked together using a tying algorithm which can bond two incompatible finite element grids with different degrees of refinement.

Finite element analysis was started from the application of inflation pressure. Then a static concentrated load was applied on tyre in vertical direction against a flat surface to simulate the contact of the tyre with road surface. The finite element ABAQUS code, was used in this work to develop models for investigating the effects of the variation of the belt angles on the mechanical behaviour of the tyre. To achieve this goal, three belt angles ($\pm 18^{o}$, $\pm 20^{o}$ and $\pm 22^{o}$ with respect to circumferential direction) were chosen for steel cords in belts. Based on the numerous trial and errors experiments carried out by several tyre manufacturers, belt angles selected within this range generally give optimum stiffness in the tread zone of the steel-belted radial tyres.

In addition, we aimed to study the effect of the inclusion of the tread patterns on the accuracy of the design variables via comparison of the numerically obtained results between model with simply ribbed tread and models with complex tread pattern. In these numerical experiments, four basic factors were selected including contact pressure, total strain energy (TSE), strain energy density (SED), and interlayer shear stress, as well as, tyre deformation. A comparison was also made between the computed dimension of the deflected tyre and the experimentally measured one to demonstrate the accuracy and capability of the models.

FINITE ELEMENT MODEL

A 175/70R14 84T steel-belted radial tyre was selected for this simulation. The carcass of this tyre was constructed of one body ply (polyester), two steel belts, and one nylon cap ply. ABAQUS/CAE was used as the pre-processor to generate the input file of the finite element model in this work.

The 3D finite element model was created in two stages. In the first step, finite element mesh of the axisymmetric part of the tyre body (all components except tread pattern) and tread blocks are generated separately. Then these two sets of elements are tied together using a mesh tying algorithm. In this technique two surfaces are defined as master and slave surfaces, respectively. The master surface comprises of element surfaces of the outer part of the tyre body (axisymmetric part with tread blocks). On the other hand, the slave surface includes those parts of the elements in tread blocks which are in contact with tyre body (master surface). Using the tying algorithm, the displacements of each node on the slave surface are constrained such that they have the same values of the corresponding point on the master surface [8]. The well known incremental

Table 1. Numerical values selected for material parameters in this simulation.

Material	Young's modulus (MPa)	Poisson's ratio	C_1(MPa)*	C_2(MPa)*
Nylon	3500	0.3	-	-
Polyester	9870	0.3	-	-
Steel cord	200,000	0.3	-	-
Belts, Cap ply, and Ply	-	-	0.187	0.0324
Filler	-	-	1.13	0.226
Inner liner	-	-	0.282	0.0564
Pad	-	-	0.63	0.126
Sidewall	-	-	0.187	0.0374
Tread	-	-	0.41	0.083

(*)First and second parameters of the Mooney-Rivlin equation, $W=C_1 (I_1-3)+C_2 (I_2-3)$.

nonlinear solution strategy was adopted in this work. In this technique, the solution is found by specifying the loading as a function of time and incrementing time to obtain the nonlinear response. Here, time is considered as dummy variable since the analysis was carried out under static and steady state conditions.

ABAQUS breaks the simulation into a number of time increments and finds the approximate equilibrium configuration at the end of each time increment using the Newton-Raphson method. In this numerical technique each step is restarted from the solution of the preceding step. Consequently, the effect of the loading in a previous stage on the current stage (e.g., inflation pressure on loaded shape of the tyre) is easily taken into account. Details of the complete mathematical description of this methodology and its numerical implementation can be found in literature [9].

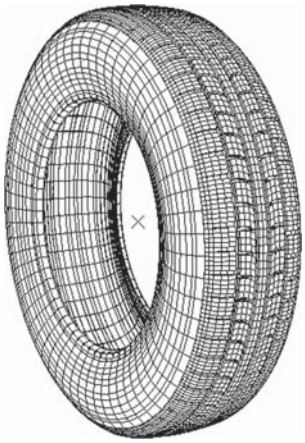

Figure 1. Finite element mesh of the tyre with detailed tread blocks.

Figure 1 shows the finite element mesh of the tyre. In this model, C3D8H and SFM3D4R elements were used. C3D8H is an 8-nodded 3D brick element with constant pressure for the definition of the rubber parts. Reinforcement materials in ply, belts, and cap ply are modelled using rebar layer in surface element SFM3DR which is a 4-nodded quadrilateral element in 3D space. Total number of elements and nodes are 26497 and 32410, respectively.

As it can be seen, despite the finite element mesh used for tyres with ribbed tread pattern in which the elements are more refined around contact zone, in the current model a uniformly discretized mesh was used. The rubber components are modelled by the Mooney-Rivlin hyperelastic and the reinforcing fibres are represented by the linear elastic material models, respectively. The Mooney-Rivlin constants (C_1 and C_2) of the compounds were determined from the uniaxial test (stress-strain) data based on the least squares fitting procedure described in literature [10].

The numerical values used for the material parameters in this simulation are recorded in Table1. The rim was assumed to be constructed from very stiff materials. Therefore, for inflation analysis, the rim and contact surface are both considered to be completely fixed. However, during contact analysis the translational degree of freedom of rim nodes in vertical direction was unconstrained so that they moved toward contact surface.

RESULTS AND DISCUSSION

All the finite element calculations were carried out

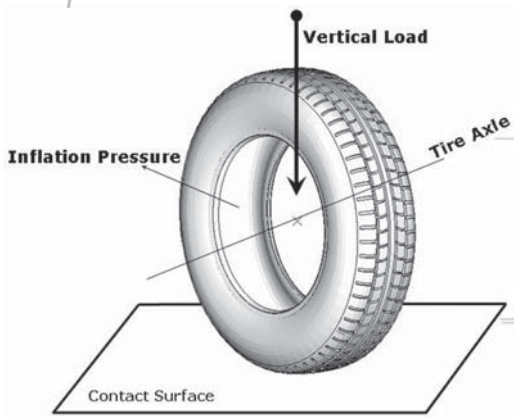

Figure 2. Schematic illustration of the loads applied on the tyre.

using ABAQUS/Standard version 6.4. The tyre is first inflated to its rated inflation pressure 0.248 MPa (36 psi). Subsequently, the rim was moved toward the contact surface incrementally up to a total load of 4900 N (500 kg). This is the maximum recommended (standard) load for a steel-belted radial tyre with load index of 84.

Figure 2 gives a schematic image of the loads which are applied on mentioned tyre. Three belt angles ($\pm 18^o$, $\pm 20^o$ and $\pm 22^o$) were selected as the design variables. All simulations were repeated for each belt angle. The deflected shape of the tyre for a sample belt angle of $\pm 20^o$ with tread blocks is shown in Figure 3.

Figure 4 illustrates the load-deflection curves at the three belt angles. As it can be seen, increasing the belt angle reduces the tyre vertical stiffness. This also results in the increasing of the ride comfort of the tyre.

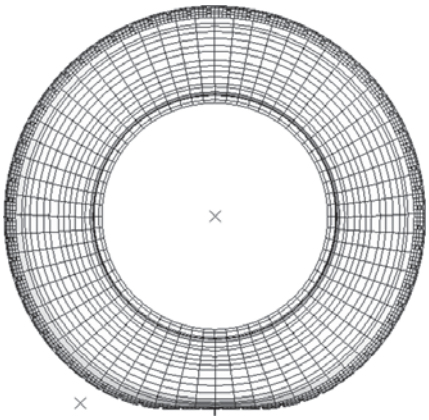

Figure 3. Deflected shape of the tyre with tread blocks for belt angle=20^o.

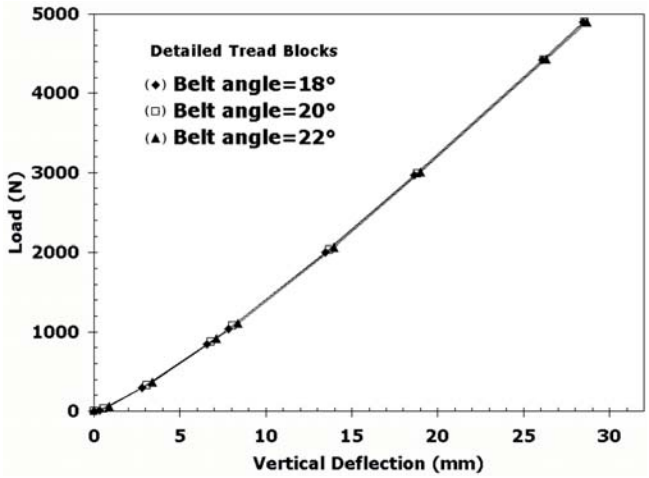

Figure 4. Load-Deflection curve of the tyre at different belt angles for model with detailed tread blocks.

The same trend was also obtained for tyre with simply ribbed tread model as shown in Figure 5.

A complete description of the finite element model of the tyre with simply ribbed tread is presented in our previous paper [11] and not repeated here. As it can be seen in both cases, the differences in vertical stiffness are not prominent. Both models predict deflection of the tyre under vertical load with belt angle of 20^o to be about 28 mm. The experimentally measured value for this parameter is 27 mm which confirms the accuracy of the developed models.

Figures 6 to 8 show the pressure field at contact zone (contact pressure), respectively. In addition, the corresponding pressure field for the simply ribbed model with belt angle of 20^o is also shown in Figure 9.

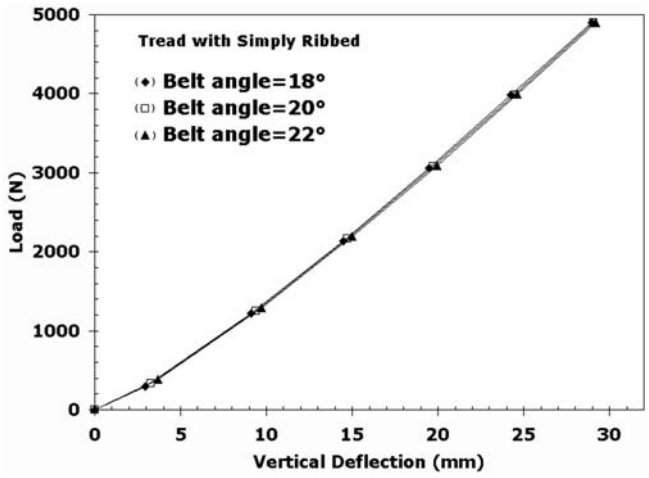

Figure 5. Load-Deflection curve of the tyre at different belt angles for model with simple tread.

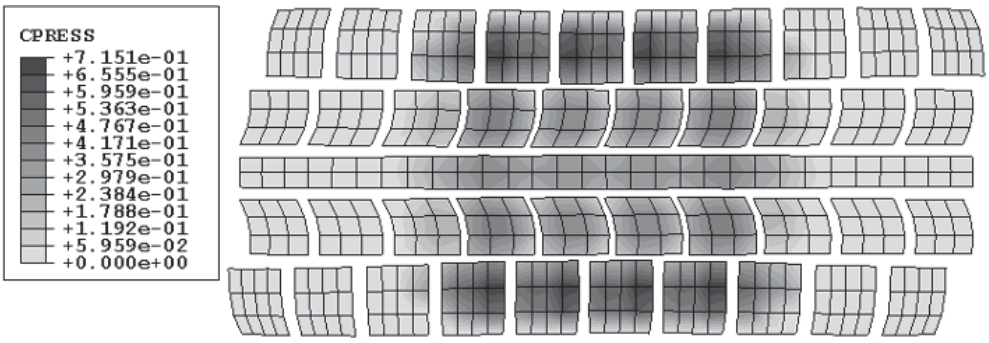

Figure 6. Distribution of the contact pressure for belt angle = 18° and model with detailed tread blocks.

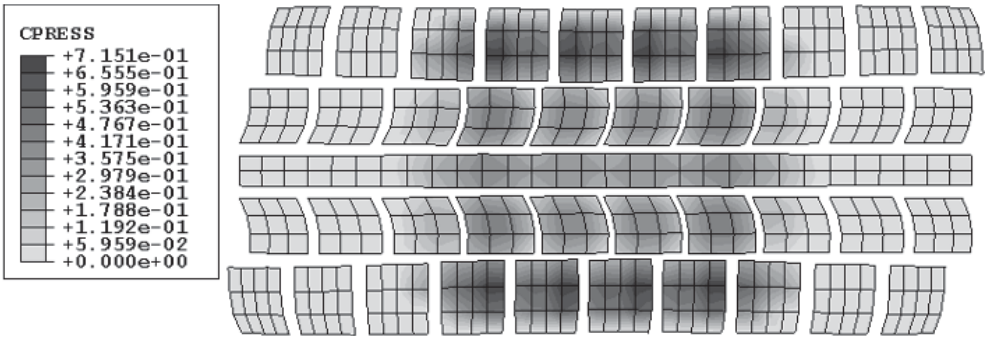

Figure 7. Distribution of the contact pressure for belt angle = 20° and model with detailed tread blocks.

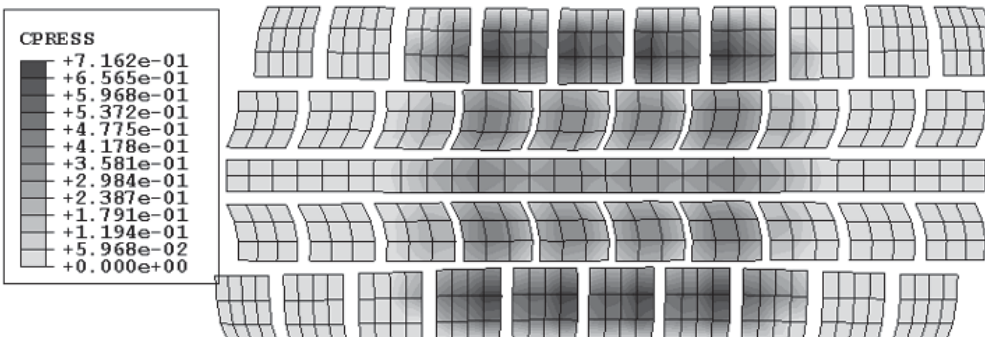

Figure 8. Distribution of the contact pressure for belt angle = 22° and model with detailed tread blocks.

In all cases the maximum pressure is located at shoulder zone which is in agreement with previously published works [12]. On the other hand, increasing the belt angle would slightly increase the maximum pressure which is due to the increase in the lateral stiffness. However, the maximum pressure in simply ribbed model is relatively lower than the corresponding model with detailed tread blocks, as can be seen in Figures 7 and 9. This is because by neglecting the detailed tread blocks, the effective contact area increases and thus the pressure which is roughly equal to the division of contact force to contact surface area, is then reduced.

The analyses performed so far were based on the assumption of a frictionless contact surface. In order to consider the effect of the friction, the analyses were repeated assuming the well-known Coulumb's friction law with a friction factor of 0.7 between tread and road surfaces.

Figures 10 and 11 show the contact pressure fields of the tyres with detailed tread blocks and simply ribbed tread, respectively. The belt angles in both cases were assumed to be equal to 20°. Comparing these pressure

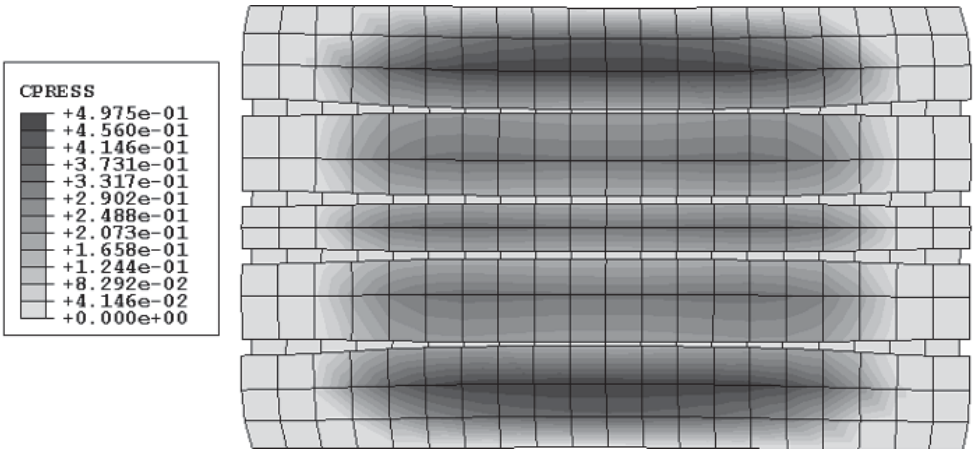

Figure 9. Distribution of the contact pressure for belt angle = 20° and model with simple tread.

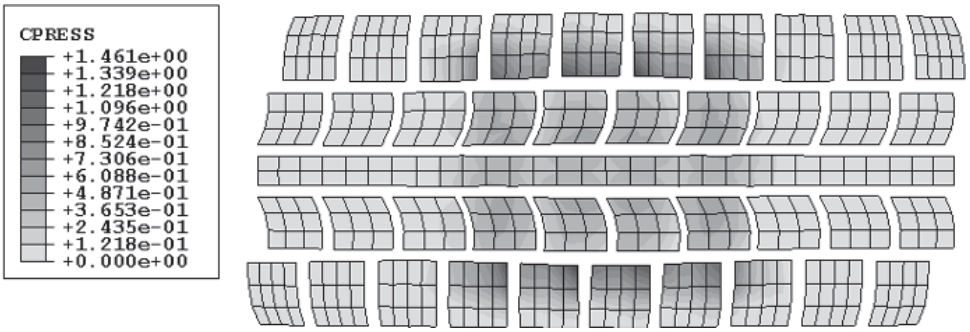

Figure 10. Distribution of the contact pressure for belt angle= 20° and model with detailed tread blocks and friction factor = 0.7.

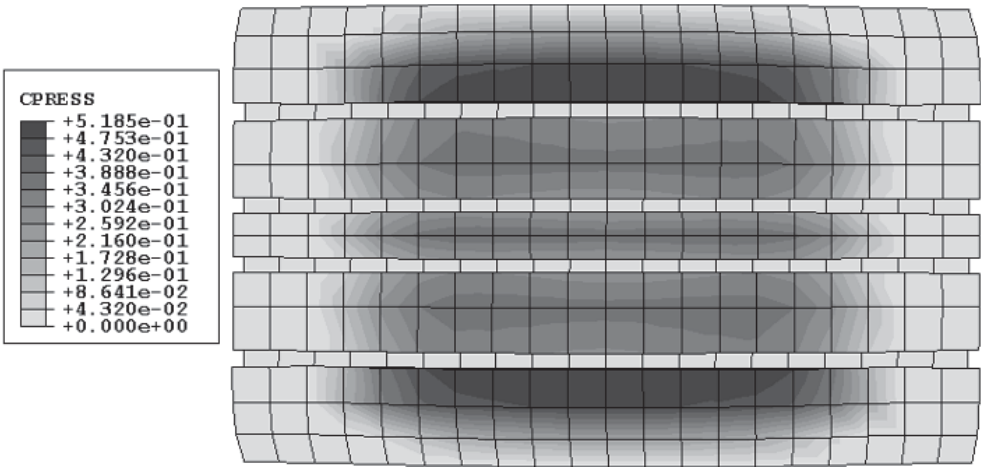

Figure 11. Distribution of the contact pressure for belt angle= 20° and model with simple tread and friction factor = 0.7.

fields with their corresponding distributions, in which it was assumed a frictionless contact (Figures 7 and 9), reveals that the inclusion of friction in the analysis leads to prediction of higher contact pressure. This is due to the increase in contact resistance between tread and road surfaces. In addition, assuming the friction in tyre with detailed blocks moves the maximum pressure from centre of the individual blocks to their edges.

Table 2. Absolute value of maximum interlayer shear stress at belt edge.

Belt angle (deg)	Interlayer shear stress (MPa) x 10^{-1}
18	6.23
20	6.15
22	6.094
20*	5.256

(*)Simply ribbed tread model.

Interlayer shear stress is another important factor in estimating tyre durability and its maximum value in all models is found to be located at belt edge zone. Table 2 gives the absolute value of interlayer shear stress in the belts edge at the centre of the contact zone. Despite the contact pressure, the interlayer shear stress decreases by increasing the belt angle. In addition, the corresponding value for simply ribbed model is lower than the same value in the tyre with complex pattern. The influence of the belt angle variation and tread blocks on total strain energy stored in the whole tyre for three mentioned model as well as the model with simply ribbed tread and belt angle of 20° were investigated and recorded in Table 3. The total strain energy stored in the model was calculated by:

$$E = \int_0^t \left(\int_V \sigma : \dot{\varepsilon} dV \right) dt \qquad (1)$$

where, σ, $\dot{\varepsilon}$, V, and t are the stress tensor, the strain rate tensor, the total volume of the model , and the time as a dummy variable, respectively. With increasing the belt angle, TSE was found to increase modestly. This is in complete agreement with the results shown in load-deflection curves presented in Figure 4. Since increasing the belt angle reduces the tyre vertical stiffness thus, the deformation (and stain) increases at a given load and the TSE increases accordingly.

Moreover, when these values were compared with the model in which the tread blocks were replaced with simple ribs, an increase in TSE was obtained. In the latter model the total volume of elements was larger than the models with detailed tread blocks. Therefore, one would obtain larger TSE in the simple model. In assessment of tyre durability, it is more common to use strain energy density (strain energy per unit volume) during the footprint loading-unloading cycles. We have selected here the maximum value of SED at belt edges as one of the most common point of failure in radial tyres. Table 4 gives these values for three mentioned models as well as the model with simply ribbed tread at belt angle of 20° and under loaded-unloaded conditions. Despite the total strain energy, SED, and its difference at belt edges during loaded and unloaded cases were reduced by increasing the belt angle. Again, the computed SED in the simple model differs notably from its associated value in complex model.

Table 3. Numerically computed values of total strain energy.

Belt angle (deg)	Strain energy (kJ)
18	52.3
20	55.3
22	58.8
20*	78.1

(*)Simply ribbed tread model.

Table 4. Numerically computed values of strain energy density (SED).

Belt angle (deg)	SED (J/mm^3) x 10^{-1}		Δ(SED) x 10^{-1}
	Unloaded	Loaded	Unloaded/ Loaded
18	1.651	2.881	1.23
20	1.676	2.810	1.134
22	1.749	2.751	1.002[1]
20*	1.994	2.439	0.445

(*)Simply ribbed tread model.

CONCLUSION

A finite element model for the simulation of the steel-belted radial tyre under static load was introduced. This model includes the details of the tread pattern and thus the interaction between tread blocks and contact surface road can be examined. Finite element calculations were carried out for three tyres with different belt angles.

These calculations were also repeated for similar tyres with simply ribbed treads. Comparing the results of contact pressure, interlayer shear stress, TSE, and SED, one can conclude that the belt angle of 20° gives the optimized values of selected design parameters. Furthermore, comparison the results of the tyre model with complex tread pattern and the simply ribbed model reveals that, although tyre deformation can be computed with reasonable accuracy by means of simply ribbed models, second order variables such as contact pressure, stress and strain energies should be calculated on the basis of the models in which the details of the tread blocks and other geometrical complexity in tyre configuration are taken into account.

ACKNOWLEDGEMENT

The author would like to express his gratitude to Kerman Tyre and Rubber Complex, Iran, for their financial support and providing technical and experimental data required to carry out this project.

REFERENCES

1. Ridha R. A., Satyamurthy K., Hirschfelt L.R., Finite element modeling of a homogeneous pneumatic tire subjected to footprint loading, *Tire Sci. Technol.*, **13**, 91-110, 1985.
2. Rothert H., Gall R., On the three dimensional computation of steel-belted tires, *Tire Sci. Technol.*, **14**, 116-124, 1986.
3. Weiss M., Tsujimoto S., Yoshinaga H., Belt construction optimization for tire weight reduction using the finite element method, *Tire Sci. Technol.*, **21**, 120-134, 1993.
4. Meschke G., Payer H. J.,Mang H. A., 3D Simulations of automobile tires: Material modeling, mesh generation, and solution strategies, *Tire Sci. Technol.*, **25**, 154-176, 1997.
5. Zhang X., Rakheja S., Ganesan R., Estimation of tire-road contact pressure distribution based on rolling finite element analysis, *Heavy Veh. Syst.*, **8**, 197-217, 2001.
6. Cho J. R., Kim K. W., Yoo W. S., Hong S. I., Mesh generation consideration detailed tread blocks for reliable 3D tire analysis, *Adv. Eng. Softw.*, **32**, 105-113, 2004.
7. Gall R., Tabaddor F., Robbins D., Majors P., Sheperd W., Johnson S., Some notes on the finite element analysis of tires, *Tire Sci. Technol.*, **23**, 175-188, 1995.
8. ABAQUS Standard Users's Manual, Ver. 6.4, Hibbitt, Karlsson & Sorensen Inc., 2003.
9. Ghoreishy M.H.R., A numerical study on the non-linear finite element analysis of a tyre under axisymmetric loading, *Iran. Polym. J.*, **11**, 325-332, 2002.
10. Finney R. H., Kumar A., Development of material constants for nonlinear finite element analysis, *Rubber Chem. Technol.*, **61**, 879-891, 1988.
11. Ghoreishy M.H.R., Finite element analysis of steady rolling tyre with slip angle: Effect of belt angle, *Plast. Rubber Compos.*, **35**, 83-90, 2006.
12. Browne A., Lumeda K. C., Clark S.K., Contact between the tire and roadway. In: *Mechanics of Pneumatic Tires*, Clark S.K. (Ed.), US Department of Transportation, Washington DC., Ch. 5, 249-363, 1981.